Available online at www.sciencedirect.com
SCIENCE DIRECT
Biochimica et Biophysica Acta 1720 (2005) 35 – 43
BIOCHIMICA ET BIOPHYSICA ACTA
BBA
http://www.elsevier.com/locate/bba

Length of C-terminus of rCx46 influences oligomerization and hemichannel properties

Carsten Zeilinger *, Melanie Steffens, Hans-Albert Kolb

Universität Hannover, Institut für Biophysik, Herrenhäuserstr. 2, D-30419 Hannover, Germany

Received 1 April 2005; received in revised form 5 October 2005; accepted 7 October 2005
Available online 5 December 2005

Abstract

Wild type connexin 46 of rat (wtrCx46), and human connexin 26 (wthCx26) and derivates from rCx46 elongated at the C-terminus by 25 amino acids (rCx46Ct) as well as C-terminal truncated constructs (rCx28.1, rCx45.3) were expressed in frog oocytes of *Xenopus laevis*. Single oocyte voltage-clamp analysis revealed that connexons or hemichannels of rCx46Ct exhibit similar conducting properties as those of wtrCx46. Insertion of a stop codon at C-terminal domains at position 243 and 409 resulted in a significant reduction in the corresponding hemichannel conductance. This result was also found for wthCx26, the shortest human connexin. Tagged connexin constructs rCx46Ct and hCx26Ct could be expressed in *E. coli* as monomers. The monomers of rCx46Ct and hCx26Ct were purified and electro-eluted from corresponding SDS gels. Studies of in vitro oligomerization showed that hexamers of these connexins were formed in presence of kinase and specific lipids. Purified rCx46Ct formed some oligomers in vitro if a lipid mixture of POPE/POPG and casein kinase I (CKI) was added, but in the presence of POPC, phosphorylated rCx46Ct monomers preferentially formed hexamers. Purified hCx26Ct formed hexamers in the presence of POPE/POPG. In addition, N-terminal truncated rCx46 (Cx35) oligomerized after phosphorylation. Reconstitution of purified recombinant connexin rCx46Ct in planar lipid bilayers mediated Ca^{2+}-sensitive single channel activity. It is discussed whether the specific C-terminal end of the expressed connexins are responsible for hexamer formation as well as channel opening.

Keywords: rCx46; hCx26 voltage clamp; Heterologous expression; Recombinant membrane protein; Affinity purification; In vitro assembly; Lipid bilayer

1. Introduction

Connexins are integral proteins of plasma membrane that oligomerize to form hexamers, the connexons, also known as hemichannels. These hemichannels form by head-to-head association between adjoining cells of metazoan cell specific cell-to-cell channels, which cluster to gap-junctions. Gap junctions allow electrical and metabolic coupling [1–5]. At least 20 connexin genes have been identified in the human genome which were cloned and biochemically as well as biophysically characterized [6]. Connexins share a common structural motif of four homologous transmembrane (TM) spanning domains, two extracellular loops between the TM regions, one intracellular loop between two TM′s and a connexin specific C-terminal cytoplasmic domain. The functional expression of connexins in oocytes of *Xenopus laevis* enables a biophysical characterization of connexin mediated connexon formation by electrophysiological techniques.

Rat connexin 46 assembles to form functional hemichannels, composed of six monomers (denoted as α3 or rCx46). Studies of the gating properties of expressed and conducting rCx46-hemichannels revealed that the corresponding voltage-dependent channel current is regulated by calcium, pH and phosphorylation [7–12]. Mutations within the C-terminal tail of rCx46 caused a loss of cellular homeostasis which seems to be linked e.g. to congenital cataract [13,14]. Although it has been suggested that regulation sites at the C-terminus are required for the physiological function of hemichannels, even truncated rCx46 exhibits conducting gap junction activity [15]. Truncation studies on Cx43 have shown that removing the C-terminus at position 242 affects the corresponding voltage-dependent gap junction conductance [16]. In comparison, human hCx26 has the shortest C-terminus of connexins. hCx26 is expressed in many tissues including the liver and pancreas. Mutated

* Corresponding author. Tel.: +49 511 762 2608; fax: +49 511 762 5916.
E-mail address: carsten@biop.uni-hannover.de (C. Zeilinger).

0005-2736/$ - see front matter © 2005 Elsevier B.V. All rights reserved.
doi:10.1016/j.bbamem.2005.10.015

connexin 26 expressed in the cochlea is associated with hearing defects [17]. hCx26 could be identified as a conducting hemichannel after expression in frog oocytes, but the expression conditions and solutions had to be optimized [18].

Since bacteria express no endogenous connexins, the bacterial system can be considered as a powerful system for providing homotypic recombinant connexins. But it is unknown whether functional hemichannels can be purified from membranes of *E. coli*, since eukaryotic posttranslational modifications are often necessary requirements for functional expression of membrane channels and their physiological function [19,20]. In this paper we studied the electrical and biochemical properties of rCx46 and hCx26 as well as C-terminal elongated and truncated constructs of rCx46 and their corresponding effects on the channel conducting properties. The frog oocyte and the bacterial expression system were used to analyze the influence of the length of C-terminus from well-known hemichannel former like rCx46 in comparison to hCx26.

2. Material and methods

2.1. Bacterial strains

The *E. coli* strains TOP10F′ and XL1 Blue (Invitrogen, Stratagene) were used to host the plasmids. *E. coli* bacteria were grown at 37 °C in Luria Bertani medium (LB) using ampicillin concentrations of 100 μg ml^{-1} if the strains were cultivated with plasmids. 1-Palmitoyl-2-oleoyl-*sn*-glycero-3-phosphocholine (POPC), 1-Palmitoyl-2-oleoyl-*sn*-glycero-3-phosphoethanolamine (POPE), 1-Palmitoyl-2-Oleoyl-*sn*-Glycero-3-[Phospho-*rac*-(1-glycerol)] (POPG) and Diphytanoyllecithin have been purchased from Avanti Polar Lipids.

2.2. Cloning and expression of rCx46Ct and hCx26Ct

The rCx46 and hCx26 genes were amplified by PCR (MBI-Taq) using the published sequence of rCx46 (NP_077352) and hCx26 (NP_003995). The sequences for the forward and reverse primers are denoted as rCx46_for: 5′-AGA TCT ATG GGC GAC TGG AGC TTC CTG G and rCx46_rev: 5′-TTC GGG CCC AAG CTT GAT GGC-3′ and hCx26_for: 5′-ATG GAT TGG GGC ACG CTG CAG-3′ and hCx26_rev: 5′- AAC TGG CTT TTT TGA CTT CCC-3′. The digested PCR-fragments were purified by agarose gel electrophoresis and cloned into the expression vector pTrcHis2A or pTrcHis2TOPO, respectively (Invitrogen) as described previously [21]. The elongation generates 25 amino acids, the anti-myc binding site followed by a histidine hexamer. The cloned products abbreviated as prCx46Ct and phCx26Ct were transferred into *E. coli* XL1-Blue cells and grown in 1.5 l of LB medium over night at an ampicillin concentration of 100 μg ml^{-1} and 37 °C. Protein expression was induced by the addition of 1 mM IPTG at an optical density (A_{600}) of 4.0, and the cells were incubated for additional 3.5 h at 37 °C.

2.3. Generation of constructs for oocyte expression

For expression of wtrCx46, and rCx46Ct in oocytes of *Xenopus laevis*, the corresponding cRNAs were transcribed by using a T7 promoter upstream of the rCx46Ct sequence added by PCR. The forward primer flanks the T7 promoter denoted as 5′-TAA TAC GAC TCA CTA TAG GGA GGA TGG GCG ACT GGA GC-3′ and the reverse primer 5′-TCA ATG ATG ATG ATG ATG ATG GTC GAC-3′ using the prCx46Ct construct (see above) as template. T7_rCx46Ct DNA was amplified by PCR (MBI Taq). Thereafter, cRNA was prepared by using a synthesis kit containing T7 RNA polymerase and CAP analogue purchased from Ambion (Austin, USA). Constructs of truncated connexins, rCx28.1, rCx45.3, have been prepared with T7 rCx46Ct forward and reverse primers Cx1228rev 5′-TTA GGC TCG TCC GCTGCTGGA-3′ Cx729 rev 5′-TTA GTG GTT GGT AAC TCC CTG CT-3, generating the constructs rCx28.1 and rCx45.3, respectively. hCx26 was cloned into the pGEMHE vector using hCx26_for: 5′-GGT ACC ATG GAT TGG GGC ACG CTG-3 and hCx26_rev and 5′-GAA TTC TTA AAC TGG CTT TTT TGA-3′.

2.4. Voltage clamp measurements

The oocytes were isolated from *Xenopus laevis* ovaries. Stage V–VI oocytes were collected and defolliculated by collagenase treatment (5 mg/ml, 355 U/mg, 1.5 h; Worthington, Type 2) in Ca^{2+}-free ND96 solution (96 mM NaCl, 2 mM KCl, 1 mM $MgCl_2$, Na–HEPES at pH 7.4 and adjusted with sorbitol to 240 mosmol/l). An injection apparatus (Nanoliter Injector, World Precision Instruments) was used to inject 23 nl of 25 ng/μl of Cx46 cRNA or 50 ng hCx26. Injections include DNA anti-sense (10 ng/23 nl) to the endogenous *Xen*Cx38 oligo 5¢-gCT gTG AAA CAT ggC Agg Atg to eliminate endogenous hemi-channel currents. Oocytes were incubated in ND96 supplemented with antibiotics (100 U/ml penicillin/streptomycin) at 17 °C.

The two-electrode voltage-clamp technique was applied to measure the expressed and conducting hemi-channels in single *Xenopus laevis* oocytes using a voltage-clamp amplifier Turbo TEC-10 CD (npi electronic, Tamm, Germany). Voltage protocols were applied by a Pentium 100 MHz Computer linked to an ITC-16 interface (Instrutech. Corp., NY). The following pulse protocol was used throughout the experiments: from a constant holding potential of −90 mV variable test potentials were applied for 10 s in the range from −110 mV to + 70 mV in steps of 10 mV after repolarization of the oocyte at a holding potential of −90 mV. The current signals were filtered at 1 kHz and were sampled at 0.5 or 0.25 kHz. Data acquisition and analysis were performed by using Pulse/PulseFit (HEKA, Germany), Igor Pro (Wave Metrics, USA), Origin (Microsoft), PatchMaschine (V. Avdonin, University of Iowa, USA). For the electrophysiological recordings the micropipettes were filled with 3 M KCl resulting in input resistances of 1–1.5 MΩ. During the current recordings the oocytes were continuously superfused with the corresponding solution at a rate of 0.5 ml/min and all recordings were performed at room temperature (20–22 °C). The standard bath was a nominal Ca^{2+}-free ND96 solution at pH 7.4. The steady-state current amplitudes were leak-subtracted and denoted as I_{ss}. The I_{ss} values are presented as function of driving voltage ($V - V_{rev}$). The leak current at the applied test potential V was determined by extrapolation of the corresponding current values in the range of −100 mV to −70 mV, at these voltages the voltage dependent hemi-channels are closed as described previously [10,12]. The reversal potential (V_{rev}) of the wtrCx46-mediated current was calculated by a 4-point interpolation using a 3rd order polynomial.

The corresponding membrane conductance G(V) was calculated from the steady-state current amplitude divided by the driving voltage ($V - V_{rev}$) and plotted as function of test potential V. In the absence of a significant time- and voltage-dependent current inactivation the corresponding G(V) values in the range of $-80\ mV < V < +70\ mV$ could be fitted by a simple Boltzmann distribution according to: $G(V) = (A/(1+\exp(-(V - V_{1/2})zF/RT)) + B)$. R, T, F have their usual meanings. $V_{1/2}$ denotes the half-activation voltage at which 50% of the maximal membrane conductance is observed. z gives the number of membrane bound equivalent gating charges. The parameter A denotes the maximal membrane conductance G_{max} of expressed and conducting wtrCx46-connexons (hemichannels) and B the corresponding leak conductance of the oocyte. B is assumed to be voltage independent. For different experiments $G(V)$ was normalised to the corresponding values obtained at $A = 1$ and $B = 0$, respectively.

2.5. Isolation of recombinant rCx46Ct and hCx26Ct from Escherichia coli cells

E. coli membranes were prepared as described previously [22]. The membranes were solubilized (1 g/100 ml) in 1% N-lauroylsarcosine, 100 mM NaCl and 50 mM Tris–HCl (pH 8.0). After centrifugation at 4000×g for 10 min the supernatant was incubated with 0.5 ml cobalt resin (Talon, Clontech). Resin was washed off with 50 ml of a buffer containing 0.5% N-lauroylsarcosine, 100 mM NaCl, 50 mM imidazole and 50 mM Tris–HCl (pH 8.0). The bound proteins were eluted in the wash-buffer containing 210 mM imidazole. Purified proteins were analyzed by SDS-polyacrylamide electrophoresis using a Tris buffered pH 8.8 PAGE system for separation gels. Samples were incubated in buffer without mercaptoethanol. After electrophoresis, the gel was either stained with Simple

Blue Safe Stain (Invitrogen) or electro blotted onto nitrocellulose. Immune-detection was performed only with anti-myc antibody coupled to alkaline phosphatase (Invitrogen) for the C-terminal tagged fusion proteins. Control blots with marker proteins (LMW, Pharmacia) or *E. coli* extract gave no background signal. Protein concentration of recombinant rCx46Ct and hCx26Ct were calculated on the basis of specific extinction coefficients for the monomers of rCx46Ct and hCx26Ct, respectively [23].

2.6. In vitro oligomerization of purified subunits

Resins containing either rCx46Ct, hCx26Ct or rCx35Ct were diluted in sample buffer and applied onto SDS PAGE. rCx46Ct and rCx35Ct were visualized by 3 M KCl [24], excised and the gel bands were transferred to electro-elution vials of the apparatus (BioRad) and eluted into a sample volume of 500 μl as described by the manufacturers protocol. To induce oligomerization lyophilized lipids POPE/POPG (1:1) were dissolved in Tris–glycine buffer and mixed with protein at a final lipid concentration of 10 mg/ml and were dialyzed against Tris–glycine buffer overnight at 4 °C until separation by SDS-PAGE. Isolated truncated rCx46Ct fragments (rCx35) obtained from the gel were dialyzed without addition of lipids. For phosphorylation 10 μg monomers (calculated on the basis of their specific extinction coefficient and absorbance at 280 nm according to [23]) were incubated with 500 U CKI, 1 mM ATP and NEB-buffer (NEB, Biolabs) for 1 h. To analyze oligomer formation, 5–10 μg from the refolded proteins were separated by SDS-PAGE without mercaptoethanol in the running buffer and preheating of the probes.

2.7. Reconstitution and measurements with planar lipid bilayer

In vitro refolded rCx46Ct (100 μg) containing POPC or POPE/POPG (1:1) was dialyzed against a 1000-fold volume excess of buffer containing 400 mM KCl and 10 mM HEPES–KOH (pH 7.4) with two changes for 36 h at 4 °C. Lipid bilayers were formed with a Teflon loop from 5 μl of a lipid solution containing 2% Lα-diphytanoyl lecithin in decane or POPC/POPE (1:1) on a 300-μm hole in a Teflon cuvette separating two 5 ml compartments (cis and trans) and electrically connected to the recording system by Ag/AgCl electrodes. The electrode of the trans-compartment was connected to the head-stage and the electrode of the cis-compartment was virtually grounded. A volume of 10 μl vesicles containing refolded rCx46Ct was added to the cis side and fused into the lipid bilayer using a solution gradient of 50 mM NaCl cis and 150 mM NaCl trans. After observation of channel activity, the solution was adjusted to symmetrically 150 mM NaCl. rCx46Ct currents mediating channel activity were measured using a low-noise current-to-voltage converter, filtered at 1 kHz with an eight-pole low-pass Bessel filter. Data were digitized using a 12-bit multifunction I/O board (PCI-MIO-16E-4, National Lab) and a 333 MHz pentium II computer and stored on a hard disk. Data acquisition and single channel analysis were performed with Lab View (Vers. 5.0, National Lab) and Origin (Vers. 6.0, Northhampton, MA) software packages.

3. Results

3.1. Molecular design of rCx46 constructs by elongation and truncation

To identify whether a sequence tag exists that is involved in hemichannel function different connexin genes were compared. An alignment shows that the lowest homology is found in the C-terminal domain. Alignment analysis of numerous connexins with wtrCx46 revealed that some connexins share homologous C-terminal ends.

Although wtrCx46 and wtrCx43 share a high degree of homology, the corresponding biophysical properties are quite different. wtrCx46 matches with those connexins that have a known hemichannel function similar to human (hCx46), bovine (bCx44), zebrafish (dCx48.5) and chicken (cCx56), but differs from frog (xCx38) and rat (rCx43) (Fig. 1).

3.2. Hemichannel conducting properties of elongated and truncated rCx46 and hCx26 constructs

Hemichannel behavior of wild-types wtrCx46 and wthCx26 and constructs of wtrCx46 derivates were analyzed by voltage-clamp measurements after heterologous expression in *Xenopus* oocytes. Fig. 2 shows single oocyte voltage-jump current-relaxation measurements and corresponding steady-state $I-V$ curves recorded for expressed wtrCx46, wthCx26, C-terminal elongated rCx46 (rCx46Ct) by 25 amino acids and truncated rCx46 at positions 243 (rCx28.1) or 409 (rCx45.3). Both the expressed wild type and elongated rCx46 mediate similar kinetics of voltage-dependent currents in nominally Ca^{2+}-free bath (Fig. 2a upper and lower left traces, Fig. 2d). Recently, it was shown that the steady-state current amplitude could be diminished by the presence of 1 mM Ca^{2+} in the bath independently of the applied voltage [10]. For both expressed constructs addition of external 1 mM Ca^{2+} caused a comparable shift of about 40 mV of the activation voltage to depolarizing voltages (Fig. 2d, corresponding $I-V$ curves). Fitting the G(V) curves of both, wtrCx46 and rCx46Ct with a simple Boltzmann function under control conditions revealed no significant difference in activation and net charge (Fig. 2e). In contrast, expression of the constructs rCx28.1 and rCx45.3 resulted in a significant reduction of the hemichannel conductance (compare Figs. 2a, b), which is obviously induced by deletion of seven or 173 amino acids apart from the C-terminus. In comparison, conditions as used for wtrCx46 were not successful to mediate hemichannel activity of wild type hCx26 (Fig. 2c).

3.3. Bacterial expression and purification of rCx46Ct and hCx26Ct

The open reading frames encoding wtrCx46 and hCx26 were cloned into the appropriate bacterial expression vectors (pTrcHis2A, pTrcHis2TOPO Invitrogen) to elongate the open reading frame of wtrCx46 and wthCx26 at the C-terminus by an anti-myc recognition site for antibody detection as well as a hexahistidine for protein affinity purification. C-terminal elongation was designed as useful tool for purification and subsequent immunological detection [22,25]. Additionally, three amino acids generated by the pTrcHis2A vector at the N-terminus. A hydropathy plot of rCx46Ct and hCx26Ct revealed four transmembrane domains TM1 to TM4, which are separated by two external and one internal loop. The additional fusion sites at the C-terminus did not cause substantial changes in the derived hydropathy profile (data not shown).

For the first time, we have used the bacterial expression system to study the consequences of manipulations on wtrCx46 and hCx26 for oligomerization to hexamers. Both constructs pTrcH2A_rCx46 and pTrcHis2TOPO_hCx26, abbreviated to rCx46Ct and hCx26Ct, respectively, were used for heterologous protein expression in *E. coli*. The tagged proteins were solubilized by 1% N-lauroylsarcosine from *E. coli* membranes

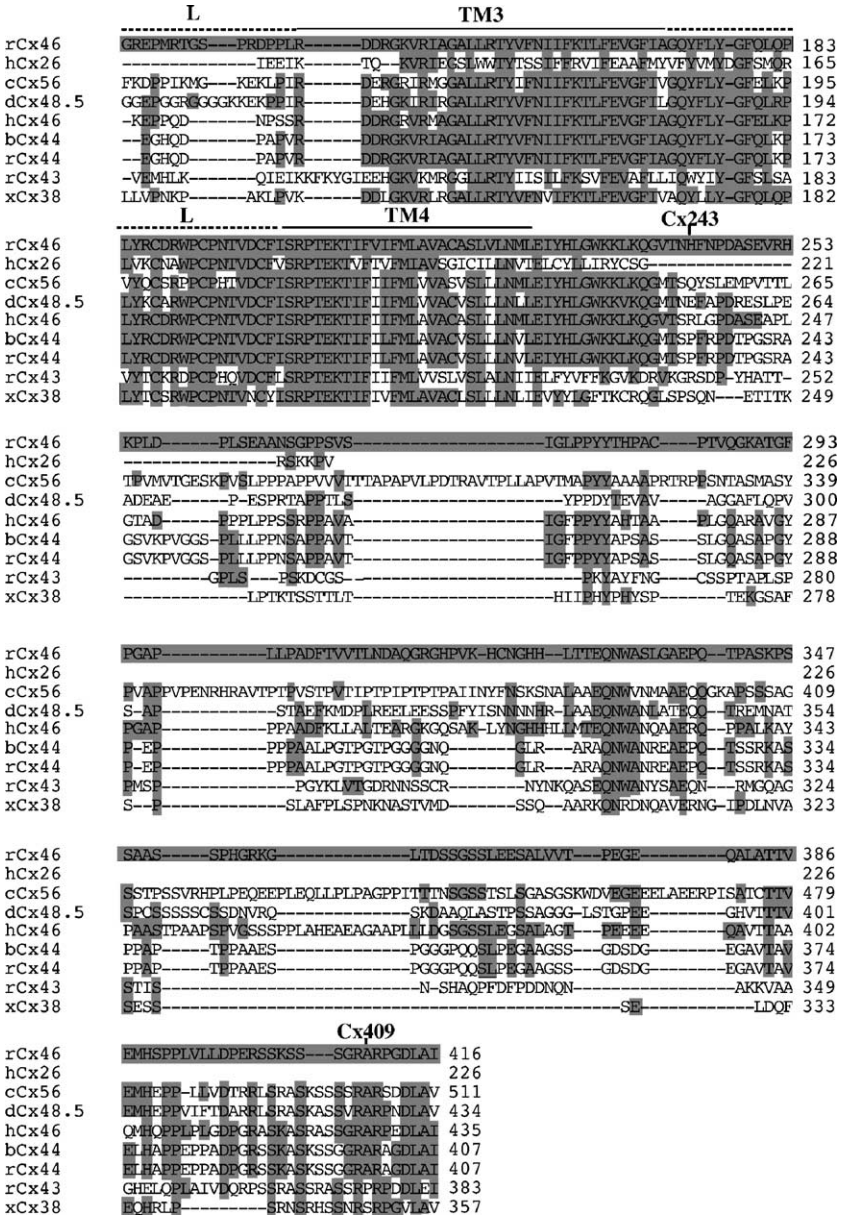

Fig. 1. Phylogenetic relationship of C-terminal ends of putative hemichannel former and other connexins. Alignment of rCx46 (*Rattus norvegicus*, NP_077352.1) with hCx46 (*Homo sapiens*, Q9Y6H8), bCx44 (*Bos Taurus*, P41987), dCx48.5 (*Danio rerio*, AF465751), cCx56 (*Gallus gallus*, P29415), xCx38 (*Xenopus laevis*, AAH43801.1), rCx43 (*Rattus norvegicus*, NP_036699) and hCx26 (*Homo sapiens*, NP_003995). The putative transmembrane domains (TM) and loops (L) are marked above the alignment. rCx46 homologous and conserved amino acids are highlighted in grey. The multiple sequence alignment was performed with DNA-Star software using the Clustal W algorithm. The predicted membrane spanning regions were obtained from DNASTAR, using the Kyte–Doolittle algorithm. Stop position of reverse primers for truncation are marked.

or inclusion bodies. The His-tagged fusion proteins were applied onto a metal chelating affinity column and purified into increased imidazole concentrations. SDS-PAGE analysis of the fractions showed that the recombinant rCx46Ct protein appears at 50 kDa, which corresponds to the expected size (49.7 kDa) of the monomer construct (Fig. 3, lane 1). Also, immune detection of the His-tag identifies a band at 50 kDa for the purified rCx46Ct protein, which confirms the expression of the correct open reading frame in *E. coli* cells (Fig. 3, lane 2). In the range of 20 kDa to 50 kDa, several further faint bands are visible. Protease inhibitors like leupeptin, pepstatin, PMSF and EDTA have been used to prevent proteolysis, but the appearance of additional bands did not change. This finding could indicate that several start codons are responsible for the appearance of accessory protein bands. In comparison, the purified protein hCx26Ct ran close to the predicted molecular mass (~30.048 kDa) of 29.6 kDa as expected for the monomer construct (Fig. 3, lane 3).

3.4. In vitro hexamer assembly of electro-eluted connexin monomers rCx46Ct and hCx26Ct

To analyze whether hexamers for both tagged connexins, rCx46Ct and hCx26Ct, can be formed from monomers the

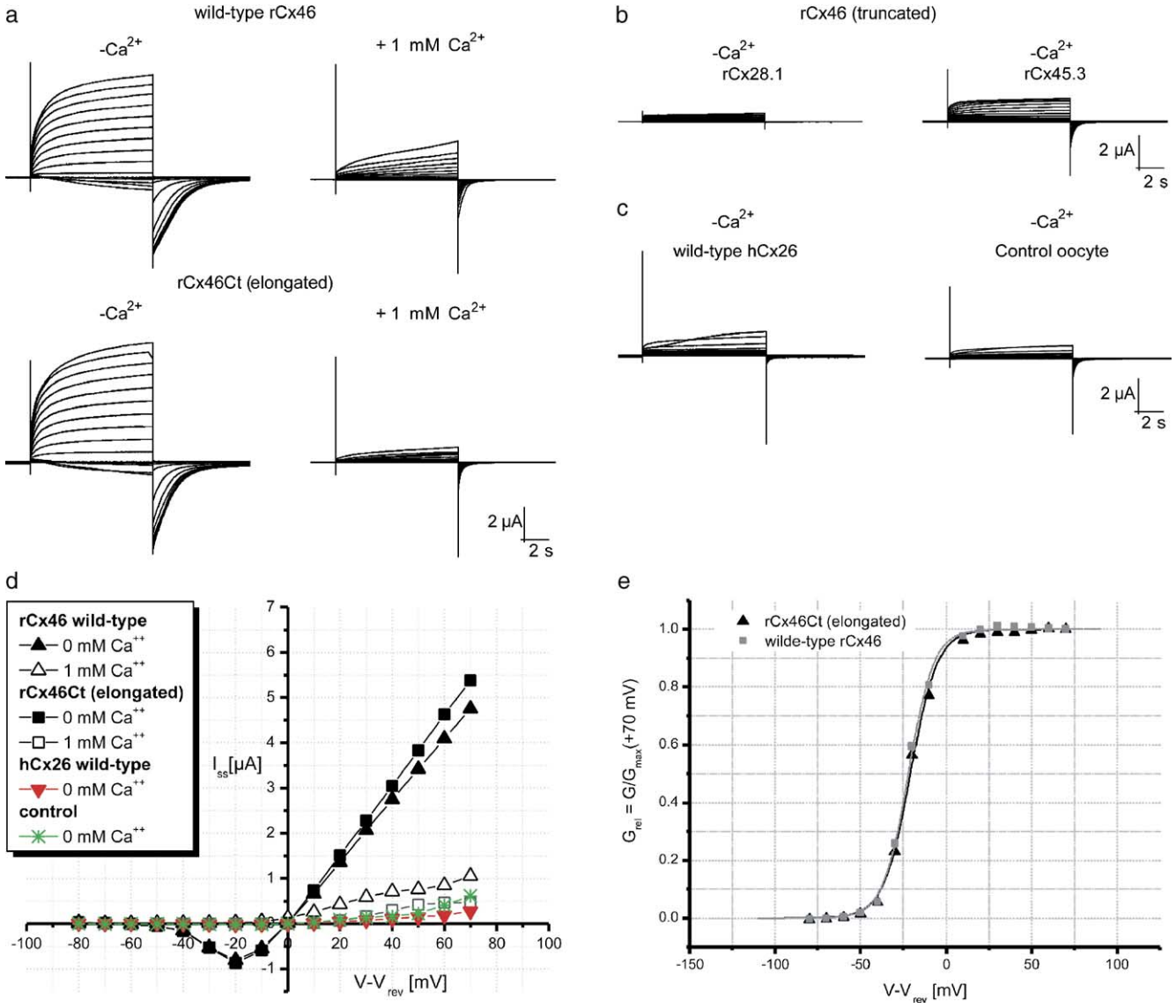

Fig. 2. Voltage-jump current relaxations recorded for various connexins expressed in single oocytes of *Xenopus laevis*, corresponding Boltzmann function and $I-V$ curves. (a) Representative macroscopic current relaxations recorded for wtrCx46 ($n=10$), elongated rCx46Ct ($n=10$) or (b) rCx28.1 ($n=7$) and rCx45.3 ($n=5$). Macroscopic currents were evoked by test potentials in the range from −110 to +70 mV from a holding potential of −90 mV in steps of 10 mV. The holding and test potential were each applied for 10 s. Repolarization to −90 mV generates inward tail currents. Current traces of wild type and elongated rCx46Ct in nominal Ca^{2+}-free bath solution (left upper and lower traces) or in presence of external 1 mM Ca^{2+} (right upper and lower traces). (b) Current traces of rCx28.1 (left) and rCx45.3 (right) in nominal Ca^{2+}-free bath solution. (c) current traces of wthCx26 (left) current traces of control oocyte (antisenseCx38 injected). (d) $I-V$ curves for wtrCx46, rCx46Ct with and without 1 mM Ca^{2+}, wthCx26 and a control oocyte, respectively, obtained from the current records and a control measurement with anti-sense Cx38. (e) Corresponding normalised membrane conductance $G/G_{max}=G(V)/G(V=+70\text{ mV})$ as function of $(V-V_{rev})$. The lines show fits of the data by a simple Boltzmann function (for details see Materials and Methods). The fit parameters are z(rCx46, ■)=3.37±0.12; z(rCx46Ct, ▲)=3.20±0.15; $V_{1/2}$ (rCx46, ■)=(−22.09±0.29) mV; $V_{1/2}$ (rCx46Ct, ▲)=(−20.87±0.38) mV.

corresponding monomers were purified from SDS-gels by electro-elution once again to provide highly purified proteins. The samples were not denatured by reduction with β-mercaptoethanol or heating before being applied to SDS gels. Separated monomers were obtained directly after SDS-PAGE. Electro-eluted protein bands migrated at the predicted molecular mass of monomers (data not shown). Purified monomers did not oligomerize even after storage in the elution buffer.

As it has been shown that phosphorylation could play an important role in oligomer formation of Cx43 [19], putative phosphorylation sites of wtrCx46 were analyzed by NetPhos 2.0 [www.cbs.dtu.dk]. Fifteen serines (S132, S249, S265, S344, S348, S351, S352, S363, S365, S366, S401, S402, S405, S406) and 4 threonines (T163, T204, T207, T341) were identified as putative phosphorylation sites. Most of the serines are located at the C-terminus. In comparison, for hCx26 4 serines (S17, S162, S219, S222) and 4 threonines (T86, T123, T186, T189) were identified.

Formation of oligomers of rCx46Ct could be induced by treatment of purified monomers with Casein kinase I (CKI) in the presence of a lipid mixture of POPE/POPG (Fig. 4a, lanes 1–4). In Fig. 4a, lane 1 the isolated rCx46Ct monomer is

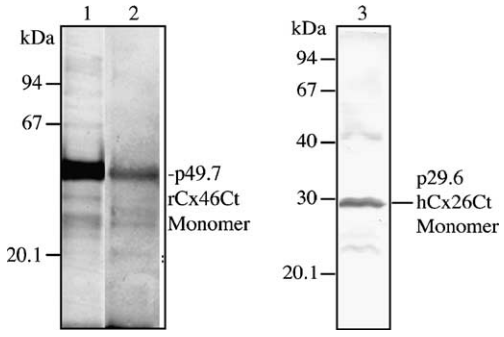

Fig. 3. Purification of rCx46Ct and hCx26Ct by metal chelating column. Lane 1: SDS-PAGE (12%, Coomassie stain) of rCx46Ct fraction eluted in 210 mM imidazole buffer, lane 2: corresponding immune detection of anti-myc tag of rCx46Ct, lane 3: immune detection of anti myc tag of purified and expressed hCx26Ct.

shown. Dimers of rCx46Ct were detected after addition of the lipid mixture, POPE/POPG or Casein kinase I (Fig. 4a, lanes 2, 3). Both, CKI and lipid treatment induced oligomer formation up to hexamers. However, higher molecular masses are hardly resolvable. If purified rCx46Ct monomers were treated with CKI and incubated with POPC (2 mg ml^{-1}) the monomers appeared at higher molecular masses. Lane 5 of Fig. 4a indicates that hexamers and oligomers with higher masses are formed and remain stable in presence of SDS. To induce oligomers of hCx26Ct the electro-eluted monomer was dialyzed in presence of POPE/POPG against Tris–glycine overnight. Monomers, trimers and oligomers of hCx26Ct could be observed in SDS-gels, but presence of casein kinase I was not required for the hexamer formation (Fig. 4, lane 6).

If the time for expression rCx46Ct in *E. coli* was longer than 8 h, a main protein band was detected at 35 kDa (p35). This mass corresponds to N-terminal truncated rCx46Ct with the first two transmembrane domains missing. This band of p35 was further purified and electro-eluted. Oligomers appeared when the SDS concentration was reduced by dialysis. Further treatment by casein kinase I induced hexamers of rCx35Ct (Fig 4b, lane 3).

3.5. Functional reconstitution of rCx46Ct

The conducting properties of reconstituted rCx46Ct were analyzed at the single channel level. After addition of 10 μl liposomes containing reconstituted rCx46Ct close to the preformed planar lipid bilayer at the trans-side single channel fluctuations were recorded at an applied voltage of −50 mV. Corresponding frequency histograms of the current amplitude for the main channel open state indicate that the channel open probability increases with negative voltages. A single channel conductance of 266±25 pS was derived from amplitude histograms (Fig. 5a). After addition of 5 mM Ca^{2+} to both sides of the planar lipid bilayer the frequency of the current fluctuations decreased rapidly (Fig. 5b). About 30 s later, a few single channel events could occasionally be identified (Fig. 5c).

Calcium is a well-known blocker of connexin hemichannel activity. This Ca^{2+}-dependent effect is in agreement with electrophysiological experiments on single oocytes expressing conducting hemichannels of rCx46Ct as shown in Fig. 2. The effect of POPC on the activity of rCx46Ct is shown in Fig. 5d. The data suggested that refolded rCx46Ct shows longer

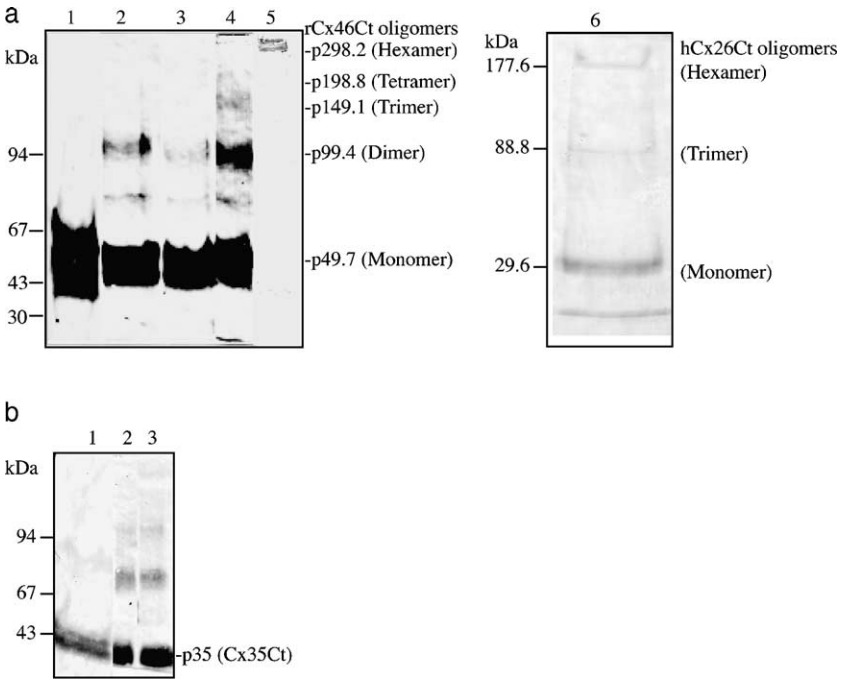

Fig. 4. Immune detection of in vitro oligomer formation of rCx46Ct, hCx26Ct and C-terminal rCx46Ct fragments. (a) Lane 1: electro-eluted rCx46Ct monomer; lane 2 after incubation with POPE/POPG 10 mg ml^{-1}; lane 3: CKI treatment; lane 4: CKI treatment and subsequent incubation with POPE/POPG; lane 5: CKI treatment followed by addition of POPC; lane 6: electro-eluted hCx26 and reconstituted in POPE/POPG 10 mg ml^{-1} after dialysis over night against Tris–glycine buffer. (b) Anti-myc immune detection of electro-eluted N-terminal truncated rCx46 (Cx35) which according to the molecular weight corresponds to tagged Cx35Ct. Lane 1, purified Cx35Ct monomer; lane 2, after dialysis; lane 3 after CKI treatment.

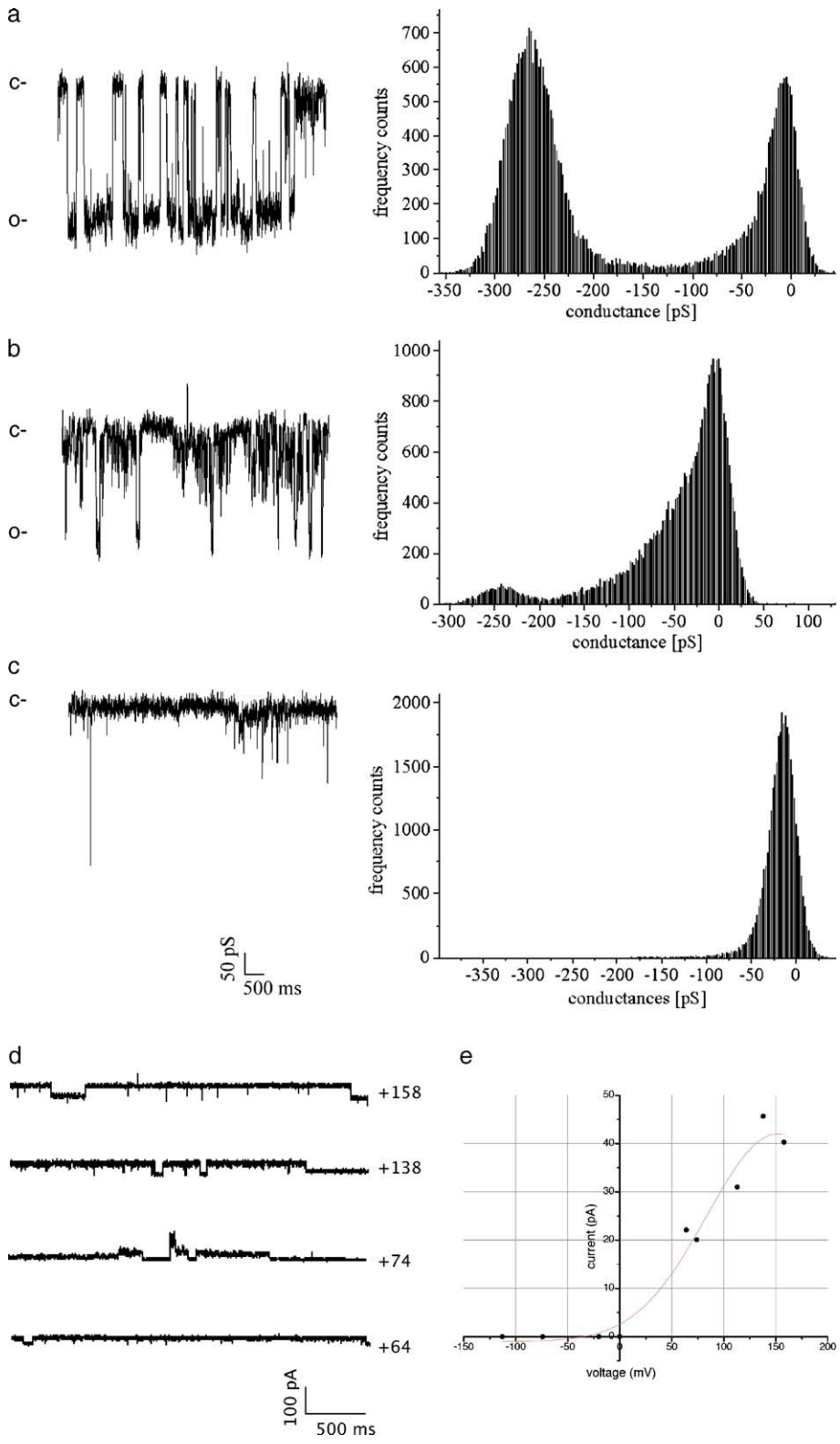

Fig. 5. Electrophysiological characterization of purified rCx46Ct after functional reconstitution into planar lipid bilayer membranes. (left) Currents recorded at −50 mV using symmetrical bath containing 400 mM NaCl, 10 mM Tris–HCl (pH 8.0). (o=open states and c=closed states). Amplitude histogram was derived from sections of 2.5–4.0 s of recorded data (right). (b) The concentration of Ca^{2+} in both chambers was adjusted to 5 mM and the current was recorded after 10 s and (c) after 30 s (o=open states and c=closed states). (d) Current traces of rCx46Ct refolded in POPC. Lipid bilayers were formed with a mixture of POPC/POPE (1:1) and corresponding $I-V$ curve (e). Vesicles (5 μl) containing purified rCx46Ct, phosphorylated with CKI and refolded in POPC were added to the cis side of the bilayer.

openings when reconstituted in POPC. Applying a negative potential did not activate rCx46Ct when vesicles containing rCx46Ct were fused into the bilayer from the cis side (Fig. 5e). A single channel conductance of 275 pS was estimated for the linear slope of the $I-V$ curve.

4. Discussion

Expression of rCx46Ct in frog oocytes revealed that the His-tagged connexin construct mediates Ca^{2+}- and voltage-gated ion currents similar to that of the wild-type rCx46 [10–12]. This finding indicates that C-terminal elongation by about 4 kDa and three additional amino acids at the N-terminus obviously has no significant effect on the conducting properties of the hemichannel. In contrast, C-terminal truncation by seven or 173 amino acids induced a significant decrease of the corresponding hemichannel mediated current after expression in oocytes. Similar observations have been found for other connexons like Cx43, since the C-terminus is suggested to be a determinant of the voltage dependence [16]. Alignment analysis of numerous connexins with wtrCx46 revealed that some connexins share homologous C-terminal ends. The high homology at the C-terminus exhibits conserved domains, which may be essential for the conducting properties of hemichannels. A hemichannel function is also suggested for dCx44 from zebrafish and for connexin44 from bovine lenses [26,27]. Our results indicate, that the last seven amino acids Arg–Pro–Gly–Asp–Leu–Ala–Ile (Fig. 1) could be responsible and a determinant for the function of the corresponding hemichannel. Furthermore, the comparison of putative phosphorylation sites revealed that the identified serine cluster is not in this section.

However, under defined conditions, hemichannel activity for hCx26 was documented in frog oocytes using high cRNA concentrations, together with a different medium and pretreatment of oocytes [18]. In our study hemichannel activity of hCx26 was not observed whereas activity of the wild-type rCx46 was documented (Fig. 2). From these functional studies together with the biochemical data, we concluded that the C-terminal domain of wtrCx46 is essential for the function of the corresponding hemichannel when expressed in oocytes. The large C-terminal domain could be a gate for channel opening. In contrast, a short C-terminal end like rCx45.3, rCx28.1 or the hCx26 channel is not functional.

We have demonstrated that the connexins rCx46 and hCx26 can be expressed in *E. coli*, which express no endogenous connexins. Our data show that *E. coli* can be used as a tool for a high yield expression of connexins. To analyze whether wtrCx46 and wthCx26 can be used for heterologous expression in *E. coli,* we used a tagged construct of both connexins, which offers the possibility to provide reliable amounts of these membrane proteins and to identify the proteins during biochemical processing. Using *E. coli* membranes only, monomers of connexin could be prepared with sufficient quantity, but did not oligomerize as hexamers, the composition of hemichannels. Previously, it could be shown that connexin monomers which were prepared from a cell-free translation system are able to form hexameric connexons [20,28,29]. For the expression system used here, connexin monomers, which were purified from SDS gels, guaranteed the highest purity of homotypic connexins. As shown previously for rCx43, we found that casein kinase I dependent phosphorylation alone did not significantly increase the formation of oligomers [19]. But our data show that both, phosphorylation and the presence of lipids, are required for in vitro formation of hexamers, whereas phosphorylation alone increased the amount of oligomers obtained from purified monomeric C-terminal fragments (rCx35Ct). This finding indicates that the first two transmembrane domains require the presence of specific lipids (POPC) to form successful hemichannels, whereas phosphorylation at the C-terminus could induce the formation of oligomers of purified C-terminal fragments. hCx26Ct monomers form hexamers in the presence of POPE/POPG, whereas rCx46Ct requires an additional treatment with casein kinase I to refold to hexamers. Obviously the C-terminal end of the different connexins is responsible for hexamer formation as well as channel opening.

To analyze whether the purified connexins can form functional hemichannels with biophysical properties of the wild type, rCx46Ct was reconstituted in planar lipid bilayers and the conductance properties were analyzed. The estimated single channel conductances of 266/275 pS are in reasonable agreement with patch-clamp experiments on frog oocytes described earlier which indicates a correct assembly of the expressed and purified hexamers of rCx46Ct [8,30,31].

The bacterial expression system appears to be a powerful method for the preparation of recombinant homotypic connexins. We suggest that in addition to rCx46 and hCx26, the bacterial expression system also be applied for other connexin types with the advantage that endogenous connexins are not present. Our data indicate that the C-terminus is essential for the assembly of connexin monomers to the hemichannel hexamer and is responsible for the corresponding conducting properties.

Acknowledgements

The authors are grateful to Dr. D.L. Paul for the supply of wtrCx46 DNA and I. Forster for improvements. Dr. C. Zeilinger was supported by the Helmholtz-Gemeinschaft, Institut für Biologische Strukturforschung, VIBS (VH-VI-013) and M. Steffens by the EU project “REFLEX”.

References

[1] E.C. Beyer, D.L. Paul, D.A. Goodenough, Connexin family of gap junction proteins, J. Membr. Biol. 116 (1990) 187–194.
[2] K. Willecke, H. Hennemann, E. Dahl, S. Jungbluth, R. Heynkes, The diversity of connexin genes encoding gap junctional proteins, Eur. J. Cell Biol. 56 (1991) 1–7.
[3] D.A. Goodenough, J.A. Goliger, D.L. Paul, Connexins, connexons, and intercellular communication, Annu. Rev. Biochem. 65 (1996) 475–502.
[4] R. Bruzzone, T.W. White, D.L. Paul, Connections with connexins: the molecular basis of direct intercellular signaling, Eur. J. Biochem. 238 (1996) 1–27.
[5] W.H. Evans, P.E. Martin, Gap junctions: structure and function (Review), Mol. Membr. Biol. 19 (2002) 121–136.

[6] K. Willecke, J. Eiberger, J. Degen, D. Eckardt, A. Romualdi, M. Guldenagel, U. Deutsch, G. Sohl, Structural and functional diversity of connexin genes in the mouse and human genome, Biol. Chem. 383 (2002) 725–737.
[7] D.L. Paul, L. Ebihara, L.J. Takemoto, K.I. Swenson, D.A. Goodenough, Connexin46, a novel lens gap junction protein, induces voltage-gated currents in nonjunctional plasma membrane of *Xenopus* oocytes, J. Cell Biol. 115 (1991) 1077–1089.
[8] E.B. Trexler, M.V. Bennett, T.A. Bargiello, V.K. Verselis, Voltage gating and permeation in a gap junction hemichannel, Proc. Natl. Acad. Sci. U. S. A. 93 (1996) 5836–5841.
[9] L. Ebihara, V.M. Berthoud, E.C. Beyer, Distinct behavior of connexin56 and connexin46 gap junctional channels can be predicted from the behavior of their hemi-gap-junctional channels, Biophys. J. 68 (1995) 1796–1803.
[10] A. Ngezahayo, C. Zeilinger, I.I. Todt, I. Marten, H.-A. Kolb, Inactivation of expressed and conducting rCx46 hemichannels by phosphorylation, Pflugers Arch. 436 (1998) 627–629.
[11] A. Pfahnl, G. Dahl, Gating of cx46 gap junction hemichannels by calcium and voltage, Pflugers Arch. 437 (1999) 345–353.
[12] B. Jedamzik, I. Marten, A. Ngezahayo, A. Ernst, H.A. Kolb, Regulation of lens rCx46-formed hemichannels by activation of protein kinase C, external Ca(2+) and protons, J. Membr. Biol. 173 (2000) 39–46.
[13] J.D. Pal, X. Liu, D. Mackay, A. Shiels, V.M. Berthoud, E.C. Beyer, L. Ebihara, Connexin46 mutations linked to congenital cataract show loss of gap junction channel function, Am. J. Physiol., Cell Physiol. 279 (2000) C596–C602.
[14] T.W. White, Unique and redundant connexin contributions to lens development, Science 295 (2002) 319–320.
[15] R. Eckert, pH gating of lens fibre connexins, Pflugers Arch. 443 (2002) 843–851.
[16] A. Revilla, M.V. Bennett, L.C. Barrio, Molecular determinants of membrane potential dependence in vertebrate gap junction channels, Proc. Natl. Acad. Sci. U. S. A. 97 (2000) 14760–14765.
[17] D.P. Kelsell, J. Dunlop, H.P. Stevens, N.J. Lench, J.N. Liang, G. Parry, R.F. Mueller, I.M. Leigh, Connexin 26 mutations in hereditary non-syndromic sensorineural deafness, Nature 387 (1997) 80–83.
[18] H. Ripps, H. Qian, J. Zakevicius, Properties of connexin26 hemichannels expressed in *Xenopus* oocytes, Cell. Mol. Neurobiol. 24 (2004) 647–665.
[19] C.D. Cooper, P.D. Lampe, Casein kinase 1 regulates connexin-43 gap junction assembly, J. Biol. Chem. 277 (2002) 44962–44968.
[20] M.M. Falk, L.K. Buehler, N.M. Kumar, N.B. Gilula, Cell-free synthesis and assembly of connexins into functional gap junction membrane channels, EMBO J. 16 (1997) 2703–2716.
[21] J. Hellmer, R. Patzold, C. Zeilinger, Identification of a pH regulated Na(+)/H(+) antiporter of *Methanococcus jannaschii*, FEBS Lett. 527 (2002) 245–249.
[22] J. Hellmer, C. Zeilinger, MjK1, a K+ channel from *M. jannaschii*, mediates K+ uptake and K+ sensitivity in *E. coli*, FEBS Lett. 547 (2003) 165–169.
[23] S.C. Gill, P.H. von Hippel, Calculation of protein extinction coefficients from amino acid sequence data, Anal. Biochem. 182 (1989) 319–326.
[24] C.E. Prussak, M.T. Almazan, B.Y. Tseng, Peptide production from proteins separated by sodium dodecyl-sulfate polyacrylamide gel electrophoresis, Anal. Biochem. 178 (1989) 233–238.
[25] J. Hellmer, A. Teubner, C. Zeilinger, Conserved arginine and aspartate residues are critical for function of MjNhaP1, a Na+/H+ antiporter of *M. jannaschii*, FEBS Lett. 542 (2003) 32–36.
[26] N. Cason, T.W. White, S. Cheng, D.A. Goodenough, G. Valdimarsson, Molecular cloning, expression analysis, and functional characterization of connexin44.1: a zebrafish lens gap junction protein, Dev. Dyn. 221 (2001) 238–247.
[27] V.K. Gupta, V.M. Berthoud, N. Atal, J.A. Jarillo, L.C. Barrio, E.C. Beyer, Bovine connexin44, a lens gap junction protein: molecular cloning, immunologic characterization, and functional expression, Investig. Ophthalmol. Vis. Sci. 35 (1994) 3747–3758.
[28] S. Ahmad, P.E. Martin, W.H. Evans, Assembly of gap junction channels: mechanism, effects of calmodulin antagonists and identification of connexin oligomerization determinants, Eur. J. Biochem. 268 (2001) 4544–4552.
[29] S. Ahmad, W.H. Evans, Post-translational integration and oligomerization of connexin 26 in plasma membranes and evidence of formation of membrane pores: implications for the assembly of gap junctions, Biochem. J. 365 (2002) 693–699.
[30] V.K. Verselis, E.B. Trexler, F.F. Bukauskas, Connexin hemichannels and cell–cell channels: comparison of properties, Braz. J. Med. Biol. Res. 33 (2000) 379–389.
[31] M. Srinivas, J. Kronengold, F.F. Bukauskas, T.A. Bargiello, V.K. Verselis, Correlative studies of gating in Cx46 and Cx50 hemichannels and gap junction channels, Biophys. J. 88 (2005) 1725–1739.